Thermal Performances of Two Different Conductivity Metal (Cu-Ag) Micro Heat Pipe of Circular Cross Section Using Different Liquids of Low Boiling Point

[1]KMN S. Iqbal and [2]M. A. R. Akhanda
[1] Dept. of Mechanical Engineering, IUBAT, Dhaka, Bangladesh
kiqbal@iubat.edu
[2]Dept. of Mechanical and Chemical Engineering,
Islamic University of Technology, OIC, Dhaka, Bangladesh.
akhanda@iut-dhaka.edu

Abstract: Electronic machines are rapidly being developed with the increasing benefits but, getting smaller in sizes resulting in more thermal stress. To manage this stress, a comparative study was conducted between a two-metal (Cu-Ag) micro heat pipe (TMMHP) and the presently utilized single-metal (Cu) micro heat pipe (SMMHP). Thermal effects of TMMHP of circular cross section at steady state were experimentally investigated. Water and three low boiling point liquids – ethanol, methanol and iso-propanol – are used as working liquids. In consideration of the usage of the actual equipment, tests are conducted by placing the heat pipe at three different orientations – horizontal, vertical and at 45_o inclination. To provide heat flux, SGW36 (Ni-Cr) electric heater-coil is coiled around the evaporator simulating the heat-generation of an actual device, and simultaneously the condenser section is directly cooled by water in an annular space. Internal fluid-flow is considered one dimensional. Ten calibrated K-type thermocouples are installed at different locations – five of them are to measure the temperatures of internal fluid and five are used to measure the surface temperatures of the tube at different axial locations. Temperatures are recorded by digital electronic thermometers. Unlike in the SMMHP, it is found that the boiling and super heat effects in the evaporator of TMMHP transform the two-phase flow into a single phase superheated vapor flow, which increases TMMHP's heat transfer capability to three and half times the capacity of SMMHP. Such an enhanced heat transfer coefficient may be possible from the improved convection which is developed from the different heat conductivity of metals that enables the TMMHP to reject heat at a higher rate through its condenser than the rate it can take heat in SMMHP through its evaporator.

Keywords: Micro heat pipe, two-metal micro heat pipe, TMMHP, circular cross section, hydraulic diameter, inclination.

Introduction

Micro heat pipe is a heat transferring device based on the phase change phenomenon of fluid contained in it. Before filling with the fluid, the container must be vacuumed to below the atmospheric pressure. MHP is considerably of small diameter, usually not over 3.0 mm [6, 18 and 25]. The micro heat pipe receives heat at one end to vaporize the fluid which is evaporator, and then travels through the next section losing no heat called adiabatic section, and terminally the condenser part through which the carried away heat dissipates to the atmosphere. Usually, micro heat pipe is made with good heat conducting metal, i.e. copper, stainless steel, nickel etc. Depending on the operating temperature range,

selected working fluids may be water or hydrocarbon compounds or it can be cesium, bismuth, sodium, lithium etc. Fluids of low boiling point (LBP) indicate here the fluids that have boiling points below the water at atmospheric pressure. A wick is shaped accordingly, and inserted within the heat pipe spanning end to end to let the condensate crawl back to the evaporator by capillary action. The wick can be made of stainless steel mesh, sintered metal powder, fiber, wire braid etc. In a micro heat pipe, the presence of sharp or non circular edges, and in other case, radially etched micro grooved inner wall of the MHP are also replacing wick that provides the capillary service. Comparing with solid metal, heat transport ability of a heat pipe of same geometry is found to be many times high at a small temperature difference. MHP's applications are widely endorsed in cooling microelectronics, nuclear reactors as far as in space satellites. Globally many researchers have been engaged in improving the MHP concepts for the last several decades; however, few of their works are cited bellow.

Study on heat pipe has been in practice since 1942 when R. S. Gaugler of General Motors, USA proposed [1]. However, heat pipe did not receive a target oriented attention until 1963 when Grover et al. [2] directed the heat pipe's condensate-returning mechanism from its confined gravitation-fed state to the simple capillary-force action of wick structure inserted in it. By the U.S. government funding, between 1964 and 1966, RCA was the first corporation to undertake research and development of heat pipes for commercial applications [3]. Starting in the 1980s Sony began incorporating heat pipes into the cooling schemes for some of its commercial electronic products instead of the more traditional finned heat sink with and without forced convection. But, it was twenty years later in 1984 when T. P. Cotter first introduced the idea of "micro" heat pipes [1]. Sreenivasa et al. [4] determined the optimum fill ratio in miniature heat pipe which indicates the same performance as the evaporator section was half filled rather than filling in full. Akhanda et al. [5] tested an air cooled condenser to investigate the thermal performance of MHPs charged with different fluids and oriented a different inclinations. Sakib Lutful Mahmood [6] at Islamic University of Technology (IUT), OIC has performed tests on different cross sections of MHP of the same hydraulic diameter charged with water at different inclinations. It was found that the best heat transfer coefficient at the circular cross section was at an angle of 90_o. Further observation was made as the thermal resistance of micro heat pipe increases with increasing of flatness ratio and its heat transfer coefficient decreases also with increasing of flatness ratio. Finally, Sakib developed an empirical equation from the experimental data and correlated all his findings which showed ± 7% nearness with the developed equation. Moon [9] used a miniature heat pipe which was squeezed in the Notebook PC to cool which may be heated up to 100_0 C. From the output of the experiment using miniature heat pipe with woven wire wicks was found to be quiet viable candidate for a stable cooling unit of Notebook P. C. Bai et al [20] experimented on loop heat pipes (LHP) under gravity assisted

operation based on two driving modes: gravity driven mode and capillarity-gravity co-driven mode, determined by a defined transition heat load. Then they compared the results with the established steady-state mathematical model. The results show the steady-state operating temperature is much lower under the gravity driven mode, and is in similar values under capillarity-gravity co-driven mode. Li et al [21] studied a ultrathin flattened heat pipe with sintered wick. The effects of each processing parameter on the thermal performance of the UTHP samples were analyzed and compared with a mathematical model incorporating effects of the evaporation and condensation heat transfer in a copper-water wick. Results indicate that the most critical factor for thermal performance of UTHP is flattened thickness, as it decreases, the heat transport capability drastically decreases and the thermal resistance increases. Babin et al. [10] developed the model that analyzes the heat transport behavior of micro-heat pipe, and presented the model of micro-heat pipe based on the analysis by Chi [11] in a steady-state operation. Longtin et al. [12] presented the improved prediction results, considering partially the shear stress in liquid-vapor interface of groove in a micro heat pipe. Swanson and Peterson [13] analyzed thermo-dynamically the heat transport phenomena in the liquid-vapor interface of heat pipe, and Wu and Peterson [14] studied the thermal performance of micro-heat pipe in an unsteady state. Le Berre et al. [15] studied experimentally the performance of a micro heat pipe array for various filling charges under various experimental conditions. The results showed that the performance of the micro heat pipe array is favored by decreasing the input heat flux or increasing the coolant temperature. Wu et al [22] investigated the use of sintered PTFE (polytetrafluoroethylene) particles as the wick material of loop heat pipe (LHP), taking advantage of PTFE's low thermal conductivity to reduce the heat leakage problem during LHP's operation. Thermal performance of a miniature loop heat pipe using water–copper nanofluid. The results of this study shows that, for high heat transfer capacity cooling devices, PTFE wicks possess great potential for applications to LHPs. Kole and Dey [16] investigated thermal performances using Cu-distilled water nano-fluid which enhanced thermal conductivity by 15% at 30_{o} C. Chiang et al. [17] developed a magnetic-nanofluid (MNF) heat pipe (MNFHP) with magnetically enhanced thermal properties. The results showed that an optimal thermal conductivity exists in the applied field of 200 Oe.

Throughout this survey, it has been found that only a single metal or bimetal alloy has been used to manufacture the heat pipes including its varieties of isometric geometry. In these cases, heat transfers occur only at constant heat conductivity at both ends of MHP for being it a single metal or an alloy. No individual or company has been found to have attempted on doing investigation on a variable heat conductivity micro heat pipe. Thus, a two-metal micro heat pipe (TMMHP) made with two different metals (i.e. Cu and Ag) of closer heat conductivity (i.e. 398 W/m-K for copper and 429 W/m-K for silver) for *variable heat conductivity* has been selected by the author Iqbal [8] in his doctoral thesis. A series of

heat inputs ranging from 2W to 16 W have been supplied to the evaporator keeping the MHP at 0_o to study the heat transfer behavior of pure water along with ethanol, methanol and iso-propanol. Then it was reexamined at 45_o and 90_o positions (evaporator uphill) while the condenser was being cooled by ambient water at a constant flow-rate of 400 ml/min. At the end, the fluid temperatures within the TMMHP as well as the surface temperature at designated locations at steady state have been recorded to compare with other researchers' experimental data. To confirm the reproducibility of the data, the experiments were repeated and found to be on the same trend line. Iqbal and Akhanda [23] studied the same on convergent-divergent geometry where the heat transfer coefficient is found two times higher than that of single metal (Cu) heat pipe. Similar results are also found in the square cross section geometry [24].

Experimental Setup

The experimental set up is essentially consisting of a TMMHP, a storage tank, a measuring cup, a power source and a digital thermometer. The schematic diagram of the experimental set up is shown in Figure 1.

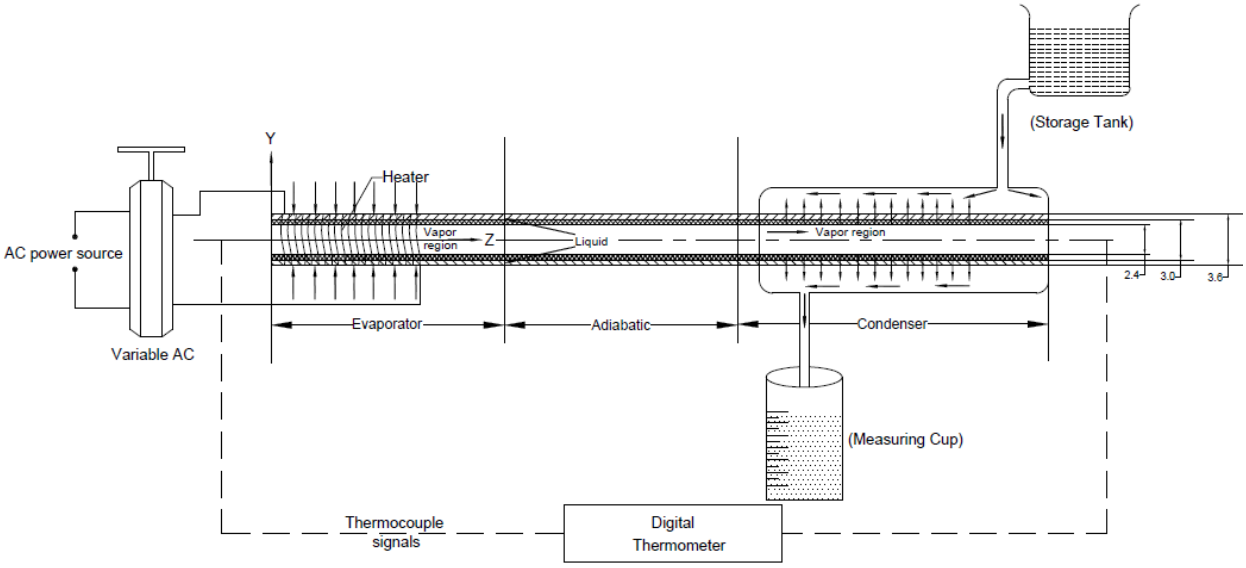

Figure 1. Schematic diagram of the experimental setup at 0_o inclination

Table 1 provides the physical dimensions of the TMMHP. The TMMHP used in this experiment is a 150 mm x 3.0 mm x 0.3 mm cylindrical metal tube which is made half with pure copper and the other half with pure silver. The copper-end is the evaporator section while the silver-end is the condenser. The lengths of the evaporator and adiabatic sections are of equal length of 45 mm each and the rest 60 mm is the condenser section. Thus, the evaporator and condenser are fully covered with copper and silver respectively while the adiabatic section is with both metals. The evaporator side is then welded to seal.

Table 1. Physical Dimensions of TMMHP (Circular)

Specifications	Dimensions	Materials
Heat pipe total length	150 mm	Copper & Silver
Evaporator section length	45 mm	Copper
Adiabatic section length	45 mm	Copper & Silver
Condenser section length	60 mm	Silver
Heat pipe inner diameter	3.0 mm	
Heat pipe outer diameter	3.6 mm	
Heat pipe wall thickness	0.3mm	
Mesh number of wick	7 holes per cm	
Wick thickness	0.3 mm	
Working fluid	Methanol, Ethanol, Iso-propanol and Water	
No. of circumferential heater in the evaporator section	1 [SGW36]	
Insulating material	(45 + 45) mm	Asbestos rope

As for wick, a steel mesh of 0.3 mm thickness with the equal length of TMMHP has been wrapped around a mandrel and inserted into the tube so that the wick radially press fit the inner wall of the tube.

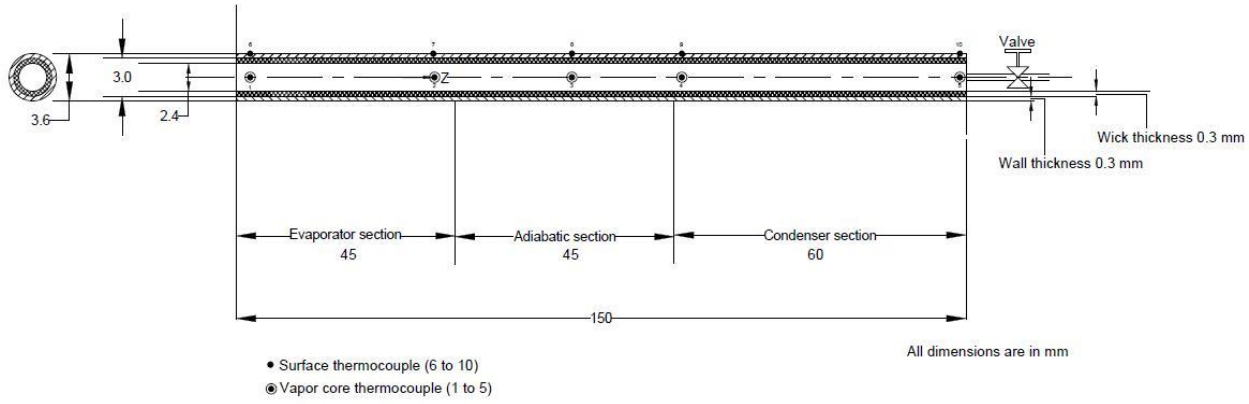

Figure 2. Positions of thermocouples along the TMMHP

Five 1.1 mm holes are drilled according to the Figure 2. Five copper constantan (K-type) thermocouples have been inserted to reach the vapor core and brazed with silver to know the internal working fluid's state. Then another five thermocouples have been attached right beside the holes by quick fixing adhesive to measure the surface temperatures at those locations. The condenser-end of the heat pipe is then plugged into one end of a capillary tube while the other end is attached with a vacuum pump. When pressure within the heat pipe goes well below the atmospheric pressure, then lock for a couple of minutes to reconfirm its air freeness. Then a pinch- clip is used to choke the capillary tube near the junction, and a slim syringe (Dispovan, 1 ml) filled with 0.5 ml of distilled water, which is 100% (Fill Ratio) of the

empty space of the evaporator, is injected into the capillary tube. Actually, the water is sucked into the capillary tube spontaneously because of having lower than atmospheric pressure within the tube. After filling, the condenser-end of the TMMHP is now pinched and sealed by brazing.

At the evaporator, a fire and electric shock proof tape has been laid around and then 36SGW nichrome heater wire has been coiled out at a closer pace possible without clinging to each other. To avoid the dispersion of heat produced by the heater in view to keep the heat input value significantly unaltered, the coil was insulated by the asbestos rope by many folds and was extended up to the end of adiabatic section. Finally, another strip of insulating tape was wrapped around to avoid getting soaked by the splash of water. Now the condenser-end of the TMMHP is wrapped up with cotton and inserted into a plastic container which has two outlets. Then the outlets are connected with flexible water tube—upper one is fitted with the valve of the coolant (water) reservoir and the lower one is dipped into an empty bucket to collect the used coolant.

The whole setup is then mounted on a rig which is placed on a wooden table. All the thermocouples have been calibrated and found with ±0.1 degree Celsius variations. Then the thermocouples have been connected with a digital thermometer through a selector switch. The coolant reservoir is filled with the supplied water which is placed above the level of TMMHP. To produce the variable heat input for the heat pipe, a Variac has been introduced, which is then monitored by one ammeter and one precision voltmeter to record the current and voltage simultaneously.

Test Procedures

At first the coolant flow is opened to run through the condenser end to ensure the condenser jacket is soaked and fully immersed with water. Then the Variac is connected with the AC power source to produce controlled heat by the heater. The power range is chosen from 2W to 16W producing heat flux ranging 4.7 kW/m^2 to 37.7 kW/m^2 simulating the generated heat in a laptop computer processor and similar electronic equipment [6]. It can be noted, before wrapping the heater coil, its red-hot power limit is checked and found to be 24W. Thus, the upper limit of 16W is quite safe for the experimental purposes. Initially, the TMMHP is inclined at 0^o (horizontally), and the time and temperature at the evaporator are recorded until the system reaches steady state. The experiment is continued by keeping the setup at 45^o and 90^o with evaporator uphill position. To attain steady state, a minimum coolant flow rate of 400 ml/min or 70 ml/s has been found to be reasonable to find the used coolant temperature equal to ambient. Although the initial steady-state for 2W is achieved not until ten minutes; however, the subsequent steady-states takes only third of the time or less than three minutes.

Results and Discussions

Using gathered data in this investigation various curves are plotted as shown from Fig. 3 to Fig. 22. Figure 3 shows time required for reaching steady state temperature for different working fluids. It is found that water takes the least time out of four liquids while the other three delayed approximately the same period of time. Ethanol and iso-propanol are almost entwined in terms of temperature rise as well as attaining steady-state condition—this may occur because of their proximity of boiling points (BP). On the other hand, methanol took the longest time to reach but at a higher temperature range than the other three. It is observable that not only the methanol's boiling point is low but also is its flash point. Methanol's flash point is only 11 ^{o}C which is 5.6 degrees less than that of ethanol. This indicates the earlier boiling and condensation of methanol than other fluids, which becomes chaotic within the narrow space of the micro heat pipe. Consequently, methanol takes longer period of time to reach thermal equilibrium thus to attend steady state than that of others. Therefore, the heat capacity of a fluid not only depends on its thermophysical properties (i.e. density, SG etc.) but also on its chemical bonding (i.e. hydrogen bonding for water).

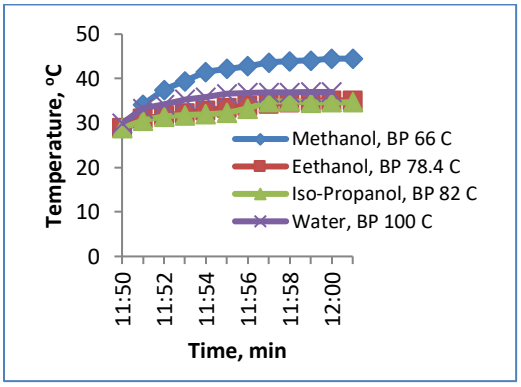

Figure 3. Time required for reaching steady-state of different fluids

The trends of temperature rises at the evaporator section for using different fluids in TMMHP are shown in Figure 4. However, water's character is specifically non-linear and on the order of three. This may happen because of the three are organic compounds and have similar chemical bonding, and the water as an inorganic compound is made up from hydrogen and oxygen's covalent bond.

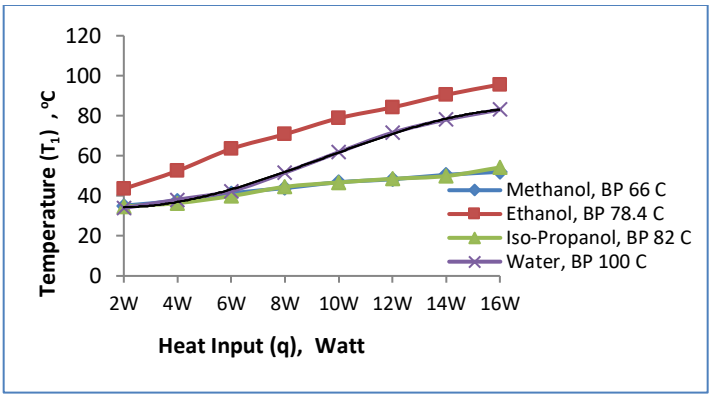

Figure 4. Rise of fluid temp. vs. heat input at the evaporator

Evaporator as a super heater

Distributions of temperatures along the length of the TMMHP for different working fluids, for different heat inputs, and also for different inclinations are shown from Figure 5 (a) to 12 (b). It is observed from these figures that in each case of fluid used in TMMHP, there is a temperature rise in the evaporator from T_1 to T_2. Annamalai A. S. *et al.* [7] has reasoned that "In the evaporator zone heat is supplied by an electric coil and the coil surface area density is very high in the middle of the evaporator portion and hence the temperature of the vapor in the middle of the evaporator is high". Authors opine different from Annamalai that there should be no reason to windup the heater coil densely in the middle of the evaporator rather wrapping must be uniformly done so the produced heat flux remains constant throughout the evaporator. Based on this work and the work of Sakib [6] and Sreenivasa [4], the working fluid should be filled only equal to or less than the empty space (vapor core) of the evaporator of the heat pipe. However, a lot more space in the heat pipe is still vacant to travel during operation. Soon after the MHP goes on operation, boiling starts at the beginning of the heat pipe—part of the fluid evaporates—that leaves a significant room empty within the evaporator which is fully wrapped up by the heater coil. Therefore, when the saturated vapor advances, it continuously receives heat from that part of heater to become superheated, and then it enters the adiabatic section. That's why we notice the temperature rise at point T_2, hence this end of the evaporator act as a *super heater*.

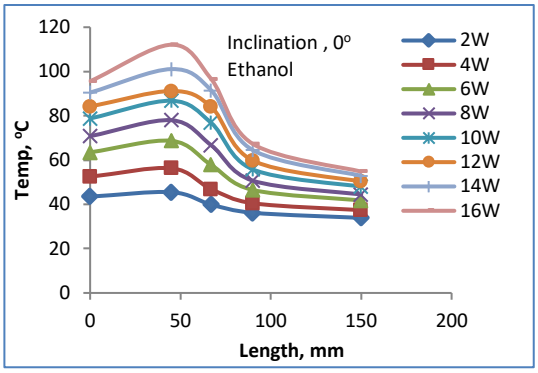

Figure 5 (a). Fluid temp. distribution along the TMMHP

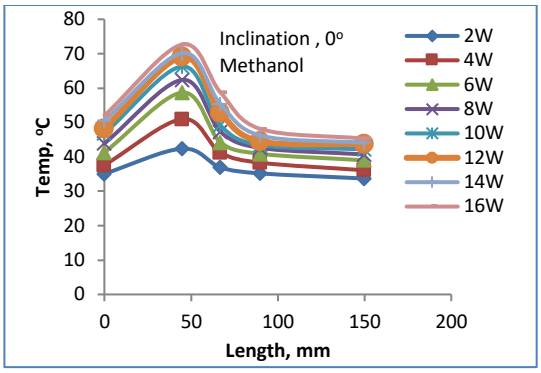

Figure 5 (b). Fluid temp. distribution along the TMMHP

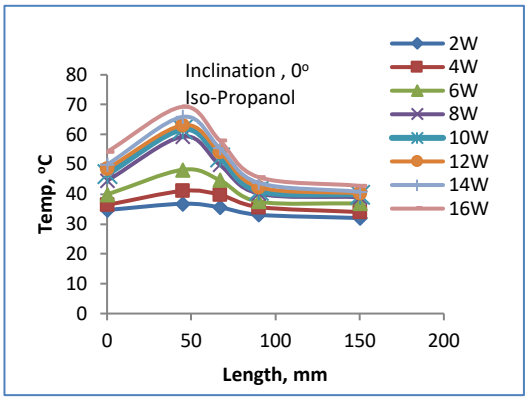

Figure 5 (c). Fluid temp. distribution along the TMMHP

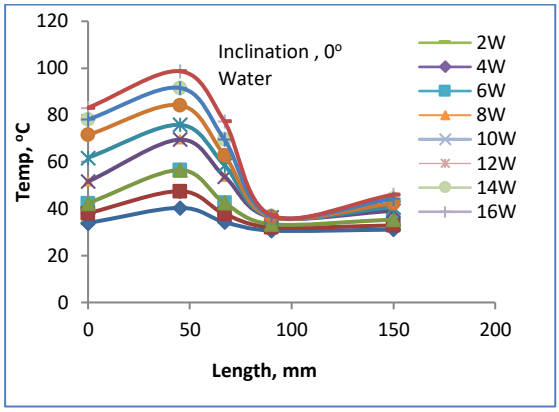

Figure 5 (d). Fluid temp. distribution along the TMMHP

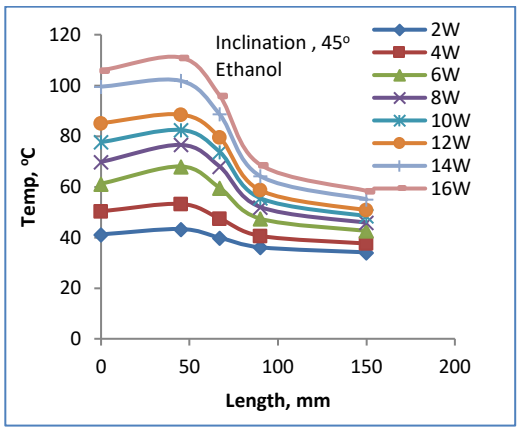

Figure 6 (a). Fluid temp. distribution along the TMMHP

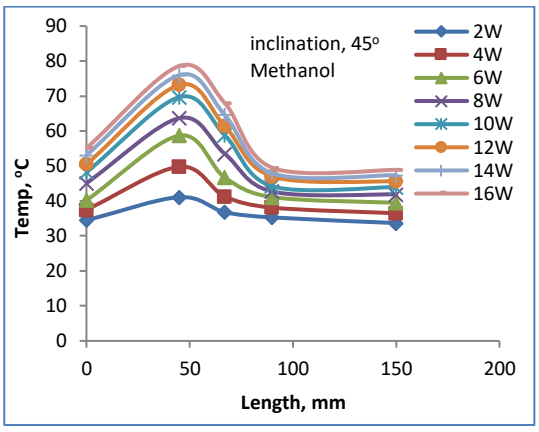

Figure 6 (b). Fluid temp. distribution along the TMMHP

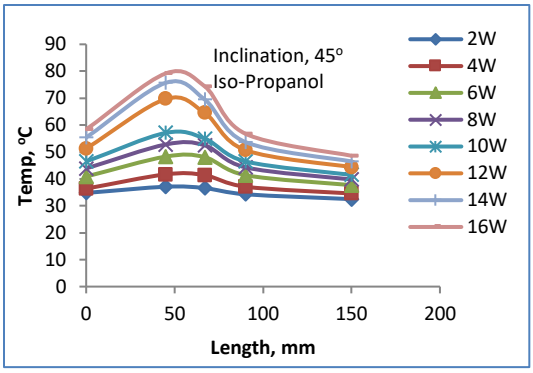

Figure 6 (c). Fluid temp. distribution along the TMMHP

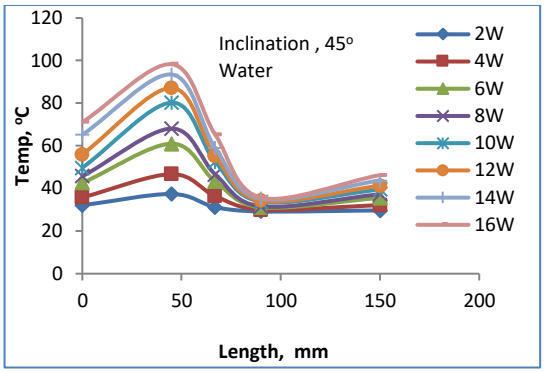

Figure 6 (d). Fluid temp. distribution along the TMMHP

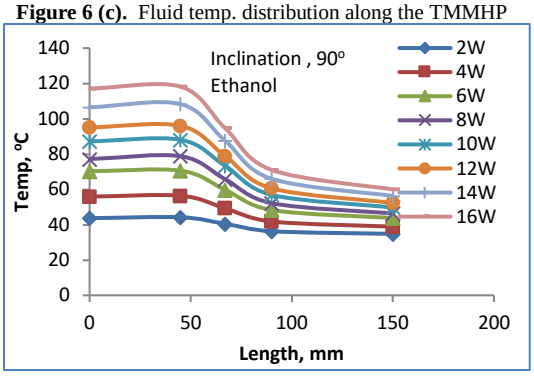

Figure 7 (a). Fluid temp. distribution along the TMMHP

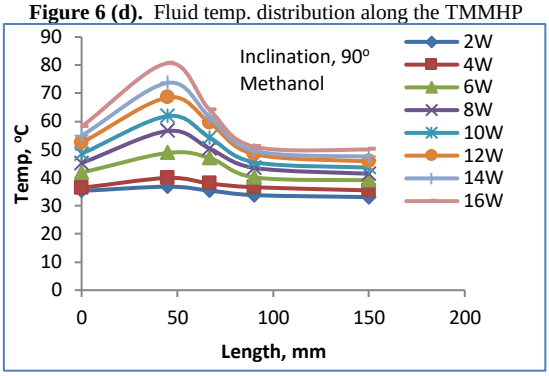

Figure 7 (b). Fluid temp. distribution along the TMMHP

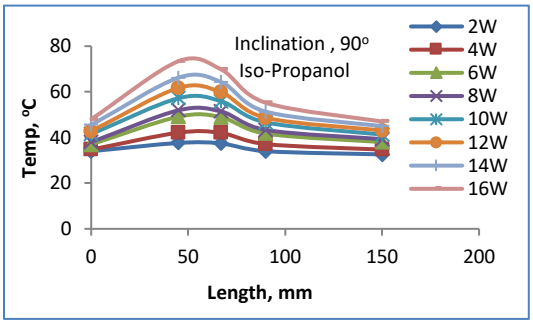

Figure 7 (c). Fluid temp. distribution along the TMMHP

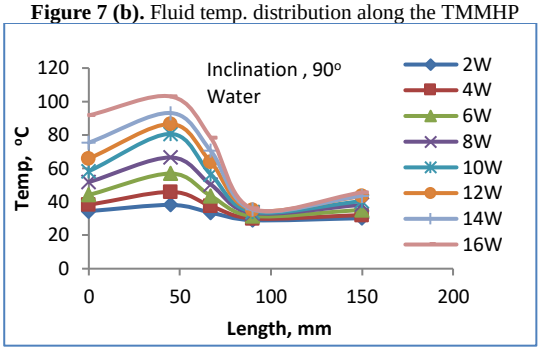

Figure 7 (d). Fluid temp. distribution along the TMMHP

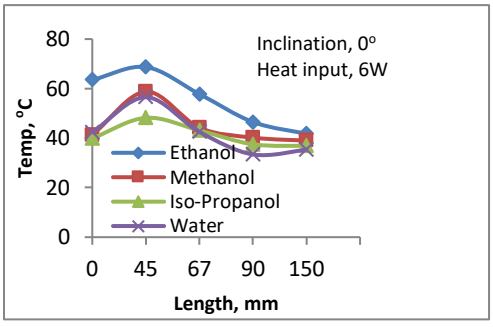

Figure 8 (a). Temp. distribn. along TMMHP for diff. fluids

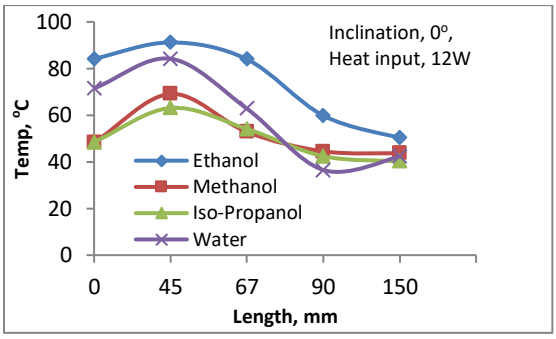

Figure 8 (b). Temp. distribn. along TMMHP at diff. fluids

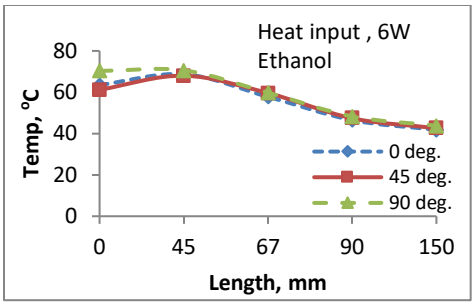

Figure 9 (a). Temp. distribn. along TMMHP at diff. incln.

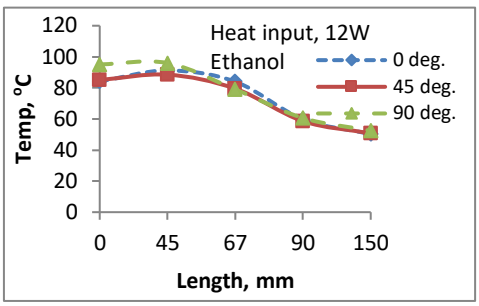

Figure 9 (b). Temp. distribn. along TMMHP at diff. incln.

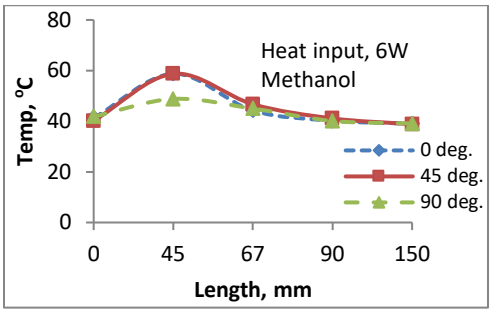

Figure 10 (a). Temp. distribn. along TMMHP at diff. incln.

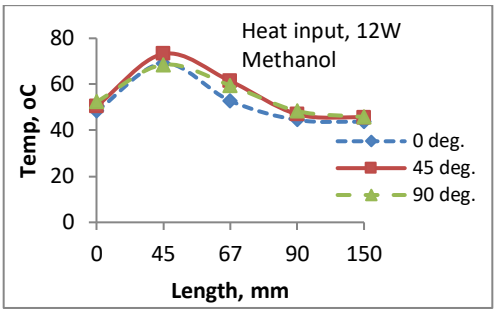

Figure 10 (b). Temp. distribn. along TMMHP at diff. incln.

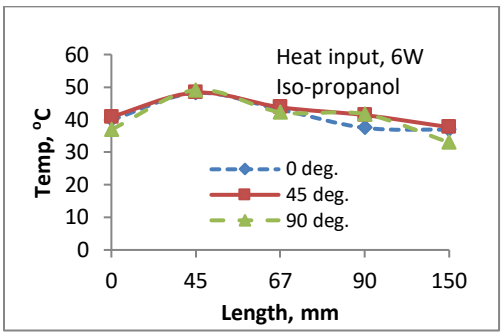

Figure 11 (a). Temp. distribn. along TMMHP at diff. incln.

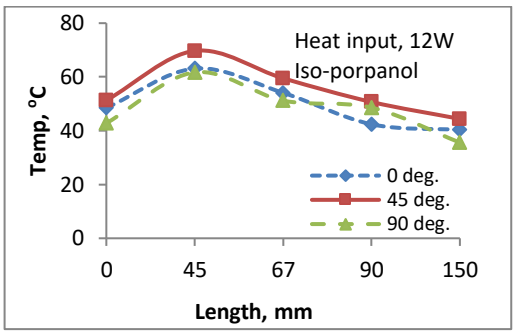

Figure 11 (b). Temp. distribn. along TMMHP at diff. incln.

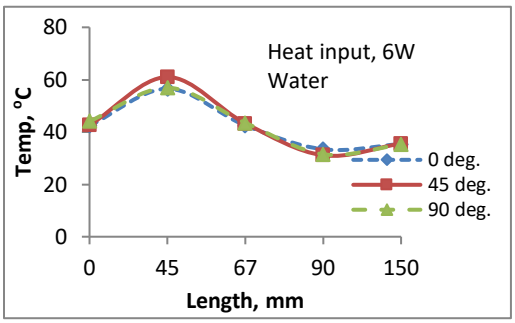

Figure 12 (a). Temp. distribn. along TMMHP at diff. incln.

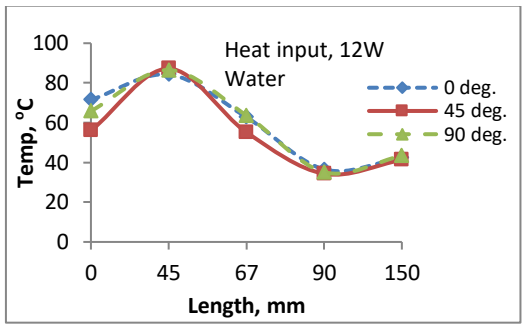

Figure 12 (b). Temp. distribn. along TMMHP at diff. incln.

Regarding the change of temperature in the evaporator, a comparative relationship between the fluids in the TMMHP and in the SMMHP [6] is shown in Figure 13. Temperature rise for methanol is found to be higher than those of other three fluids; however, they all are polynomially developed and found to be the best fit on the order of six. It is obvious that the boiling points of the fluids play an important role in superheating—the higher the boiling point, the complexier the function is. On the other hand, in the case of SMMHP [6, 7] the trend is negative which indicates no superheating effect present in it.

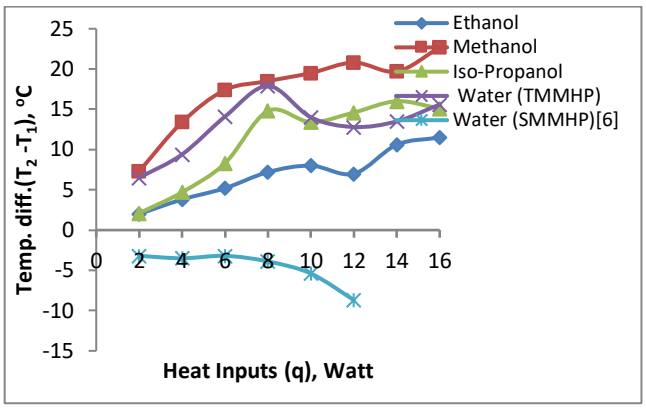

Figure 13. Comparison of temp. diff. (T_2-T_1) of TMMHP of difft. fluids with the SMMHP [6] at incln. of 0_o

Since the coolant flow rate remained constant throughout the experiments, the condensation of the fluids must be depended on the specific heat capacity of them, thus their value must vary. It is noticed the temperature rise of all fluids are maintaining their own tracks with an almost certain pace. Methanol has given the highest rise while ethanol the minimum. However, the lowest rise of temperature of ethanol may be explained as its earliest evaporation and speedy escaping the evaporation chamber due to pressure rise.

Figure 14 indicates that water was condensed within the smallest temperature band because of the highest specific heat (C_p). Considering this, methanol should have possessed the largest bandwidth, but it is found that ethanol has got the highest bandwidth. Thus it is proved again that the heat capacity of a liquid is not only depended on its physical property but also on its chemical property (i.e. structural bonding).

While being condensed, the internal working fluids were experiencing negative temperature gradient within the condenser, but the water is an exception with a positive gradient as shown in Figure 15. This behavior of water is due to the impact of the saturated liquid at the end of condenser.

The advancing water vapor from the adiabatic section towards the condensation port (T_4) creates high pressure on the saturated liquid constantly that accelerates the liquid particles of heavy momentum to hit the other end of the heat pipe.

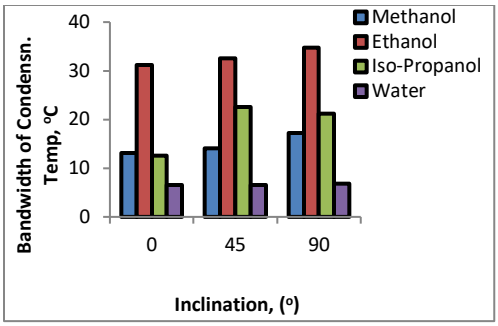

Figure 14. Band-width of condensn. temp. ($T_{4,16W}$ - $T_{4,2W}$) of diff.fluids for diff. heat inputs applied to TMMHP

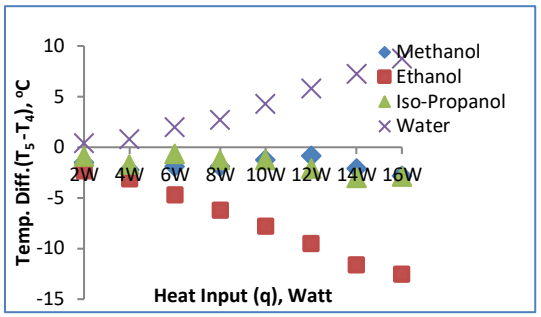

Figure 15. Comparison of condensn . temp. (T_5-T_4) range of diff. fluids for increasing heat inputs to TMMHP

.

During this impact, the inherent kinetic energy of the liquid is converted to heat, hence the temperature of the liquid increases. At the turning point, such a temperature increase of the liquid benefits the capillary action of the wick to drive back condensate even faster to the evaporator. A comparison of thermal performances between the single-metal and two-metal micro heat pipe has been established in the Table 2.

The efficiency of MHP is highlighted by its heat transfer capability at a lower temperature difference. A comparison between the TMMHP and SMMHP [6] is shown in Figure 16. As it is seen, the terminal temperature difference at TMMHP is only the fourth or even less than that of at SMMHP. This has become possible because of relatively higher conductivity of silver at the condenser port that accelerates the thermodynamic cycle of the working fluid within the heat pipe.

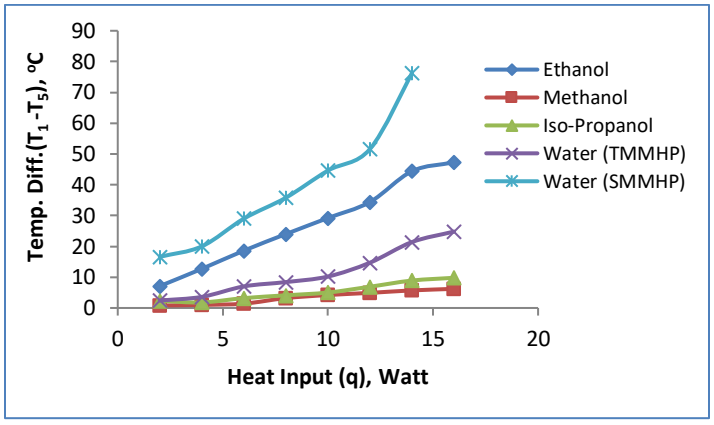

Figure 16. Comparison of terminal temp. diffs. (T_1 -T_5) of TMMHP with SMMHP [6] at 45°

Comparison of h for water between TMMHP and SMMHP

In Figure 17 and 18, *h* values of water at both SMMHP [6] and TMMHP for different inclinations can be compared. The *h* values at TMMHP are very high and sinusoidal throughout the heat input range while

the *h* at SMMHP begins with very low values and grows too slow with the increasing heat input. In addition, the highest *h* value is recorded at 90o for SMMHP and at 45o for TMMHP. However, the trajectories at both SMMHP and TMMHP clearly indicate the limit of *h* with the increasing heat input. Since all the operating and test parameters remain the same at both single and two-metal micro heat pipe, the variability of heat conductivity as well as their designed orientation in TMMHP are considered to be the only initiators for greater *h* values.

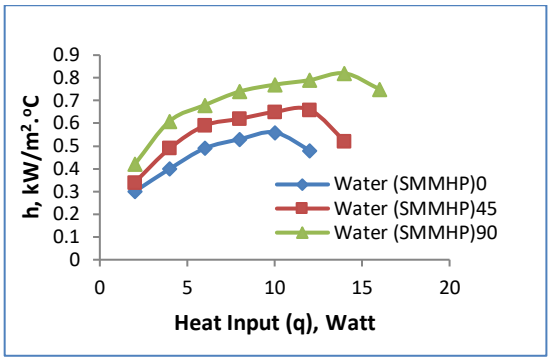

Figure 17. Convec. HT coeff. of water in SMMHP[6] at dif. inclns.

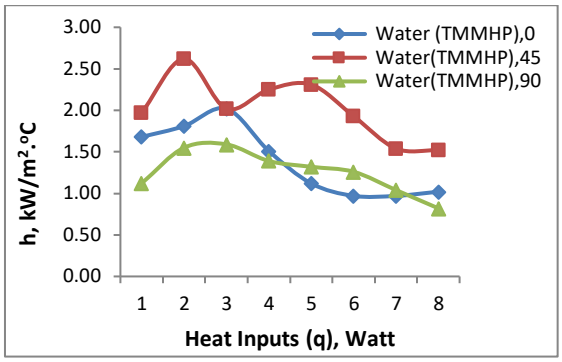

Figure 18. Convec. HT coeff.of water at TMMHP at dif. inclns.

Comparison of *h* for all fluids between TMMHP and SMMHP

Figure 19 (a), (b) and (c) show the values of heat transfer coefficient of different fluids at inclinations of 0o, 45o and 90o. In each case methanol possesses the highest '*h*' among all the fluids, and the highest value is attained at inclination 45o. Thus in respect to *h*, methanol is the most valuable working fluid out of the four for TMMHP. However, the sequence of '*h*' values for the four fluids remains the same at all three orientations.

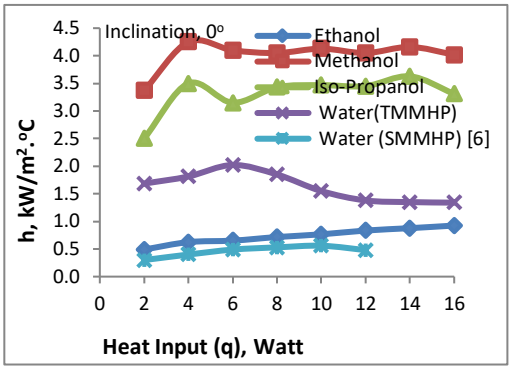

Figure 19 (a). Convec. coeff. of fluids vs. heat input in TMMHP

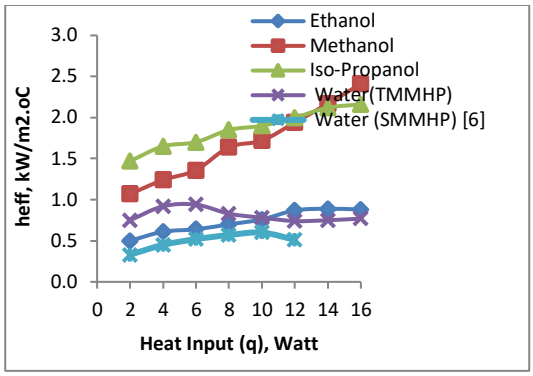

Figure 20 (a). Eff. convec.coeff.of fluids vs.heat inpu tinTMMHP

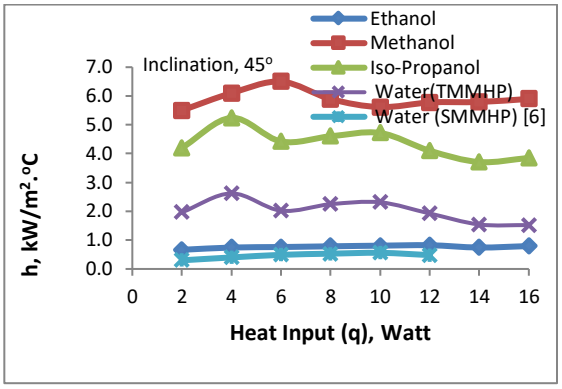

Figure 19 (b). Convec. coeff. of fluids vs. heat input in TMMHP

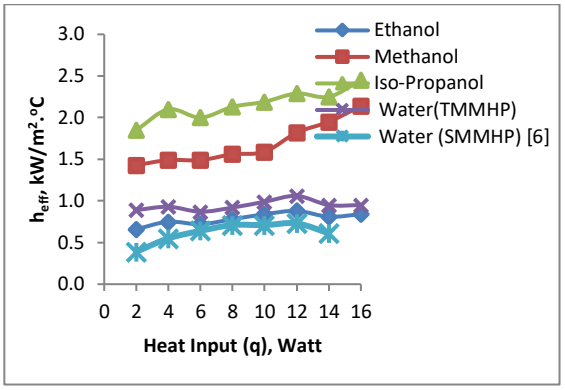

Figure 20 (b). Eff. convec.coeff.of fluids vs.heat inpu tinTMMHP

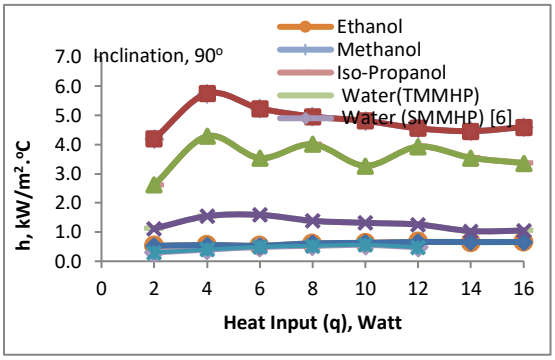

Figure 19 (c). Convec. coeff. of fluids vs. heat input in TMMHP

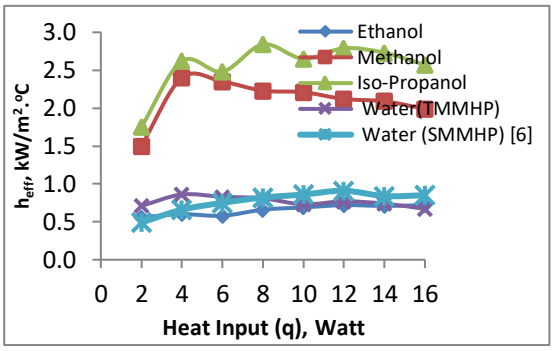

Figure 20 (c). Eff. convec.coeff.of fluids vs.heat inpu tinTMMHP

In Figure 20, the sequential rise of *h* of all four fluids in TMMHP at 45o is shown. Methanol gains the highest value of '*h*' whereas ethanol gives the lowest. Since the surface temperature of the TMMHP is depended on the heat input and heat rejection at the evaporator and condenser respectively, such extreme values of '*h*' become dependent only on the internal fluids' overall thermophysical properties. According to Newton's law of cooling, *h of a system with constant heat input and surface area gets the highest value for the smallest terminal temperature difference within the heat pipe and vice versa.* This correlation can be authenticated by comparing Figure 16 and Figure 20 where methanol achieves the highest value of *h*.

Consequently, at a small terminal temperature difference, the sharp decrease of pressure gradient leads to rapid condensation at the condenser port to increase the *h* value. As the vapor becomes liquid at the condenser, the density of the fluid therein goes many folds high. However, the *h* keeps no direct relationship with the density alone which reflects in both Figure 19 and Figure 20. Rather it is found that *h is compositely related with the fluid's density, pressure drop and heat input.* This relationship can be expressed by $h = f(\rho(p(q)))$. Then the authors have developed the dimensionless correlations from this relationship presented later.

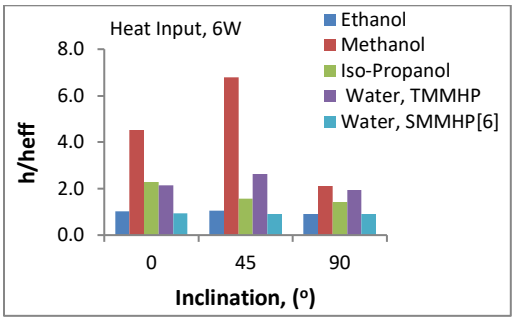

Figure 21(a). Comparison of h/h_{ef} between TMMHP and SMMHP [6]

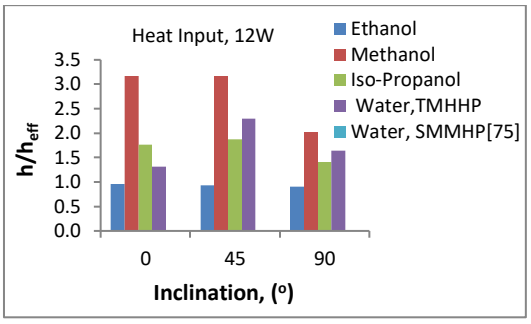

Figure 21(b). Comparison of h/h_{ef} between TMMHP and SMMHP[6]

In Figure 21(a-b), all the fluids' dimensionless heat transfer coefficients are shown including the water's h/h_{eff} at single-metal micro heat pipe. The maximum value of methanol is seen because of its lowest boiling point (66 $_{o}$C) which allows it to complete the boiling-condensation cycle faster than the other three liquids. However, comparing the water's h/h_{eff} value at TMMHP is twice as high as that of at SMMHP [6]. Thus, the two different thermal conductivities at the two ports of the TMMHP initiate the quicker heat removal than that of the SMMHP, hence improves the *h* so greatly.

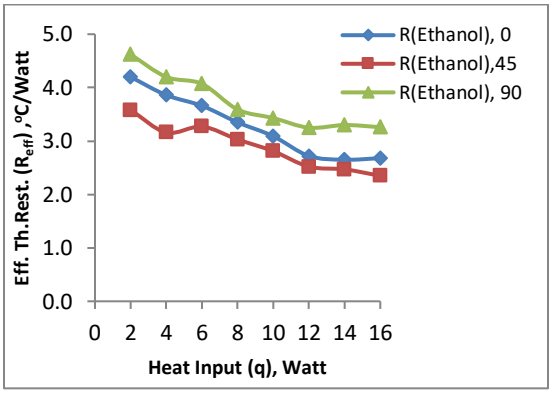

Figure 22 (a) Thermal Resistance vs. Heat input at TMMHP

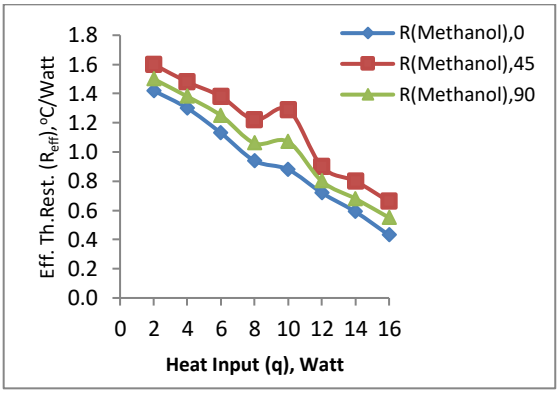

Figure 22 (b) Thermal Resistance vs. Heat input at TMMHP

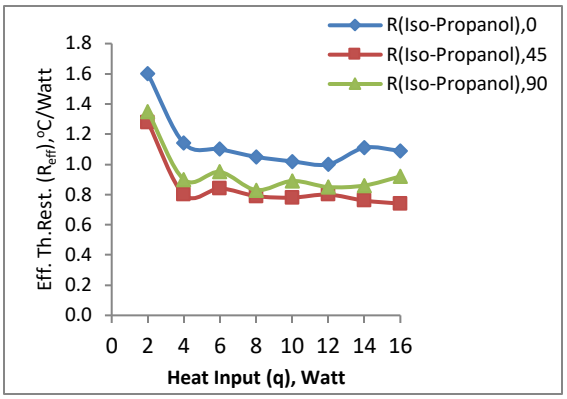

Figure 22 (c) Thermal Resistance vs. Heat input at TMMHP

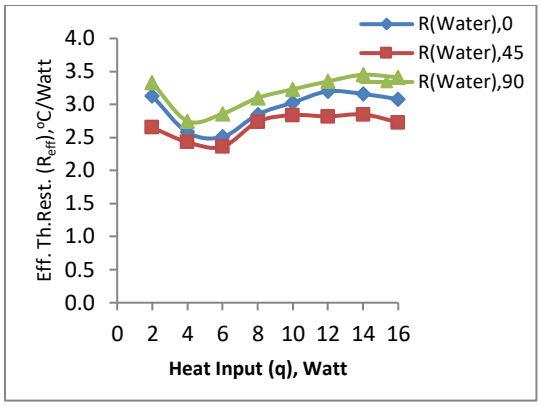

Figure 22 (d) Thermal Resistance vs. Heat input at TMMHP

In Figure 22 (a-d), effective thermal resistances are shown for all the working fluids used in the TMMHP. It is obvious that the orientation of the heat pipe plays an important role on maintaining the order of thermal resistance for particular fluid. However, except water three liquids are keeping almost the same lower trend of thermal resistance with the increasing heat input. This difference is occurred because of the two different kinds of fluids where water is covalent compound and other three are hydrocarbons. Having such difference in chemical structure, their thermophysical properties (i.e. density, specific heat etc.) also go different resulting thermal resistances. In all four cases, it is seen that like the heat transfer coefficient, thermal resistance also takes a turn as the heat input is increased to a moderately high value (i.e. 10W). Methanol is found to be of the lowest thermal resistance as 0.43 ^{o}C/Watt as it is in congruence with the highest value of *h* in comparison.

A comparison of thermal performance between single-metal (SMMHP) [6] and two-metal micro heat pipe (TMMHP) observed in this study is given in Table 2.

Table 2. Comparison of thermal performance between SMMHP [6] and TMMHP

Sl. No.	**Parameters**	**SMMHP [6]**	**TMMHP**	**Remarks**
1	Thermal conductivity (k)	Constant	Variable	Rate of heat removal is increased in TMMHP.
2	Bandwidth of condensation temperature (Water, 0^{o}incln.)	Small 33.9^{o} - 37.5 ^{o}C	Large 30.7^{o} - 36.5 ^{o}C	Condensation takes place at higher temp. in TMMHP than in SMMHP.
3	Overall temp. difference between two ends of MHP (Water, 0^{o}incln.)	41.2 ^{o}C	13.0^{o}C	In TMMHP is much smaller, thus enhances cyclic order and quick heat removal.
4	Temp. gradient at condenser for water	Negative	Positive	Positivity at TMMHP improves capillary action.
5	Time reqd. to complete cycle (Water, 0^{o}incln.)	2 min	1½ min	Because of thermal vacuum created in TMMHP.
6	h/h_{eff} (Water, 0^{o})	0.93	1.82	Overall *h* is very high at TMMHP.
7	Overall *h* (Water, 0^{o}incln.)	0.46 kW/m2. ^{o}C	1.33 kW/m2. ^{o}C	At TMMHP *h* reaches enormously high.
8	*h* with respect to increasing Q	~uniform	increasing	Mean value of *h* is **3.5** times higher at TMMHP than that of SMMHP.

Validation of the experimental setup with known results

To validate the present experimental setup and results, four experiments are carried out in the IUT Lab with another setup following the test procedures applied to TMMHP. The setup contained a circular SMMHP made with copper which was tested by the experimenters Hossain et al. [18] for ethanol, methanol and acetone, and operated at 30o, 50o, 70o and 90o angles with the heat inputs of 0.61W, 1.56W, 3.67W, and 8.71W. Out of three fluids, ethanol is selected as the working fluid for the validation test. The specifications of the setup are given in Table 3.

Table 3 Specifications of the experimental setup

Test Parameters	Dimensions (mm)
Outer diameter of the tube, d_o	2.0
Hydraulic diameter of the tube, d_h	1.8
Length of heat pipe, L	150
Length of evaporator section, L_e	50
Length of adiabatic section, L_a	30
Length of condenser section, L_c	70
Inclinations	30o, 50o, 70o ,90o(vertical)

The values of overall heat transfer coefficient, *U*, obtained from the source [18] are compared with those found from the validation experiment, which are within the proximity of 93% of TMMHP. Similarly, the thermal resistances, *R*, are also compared and found to be within 95% of the known values.

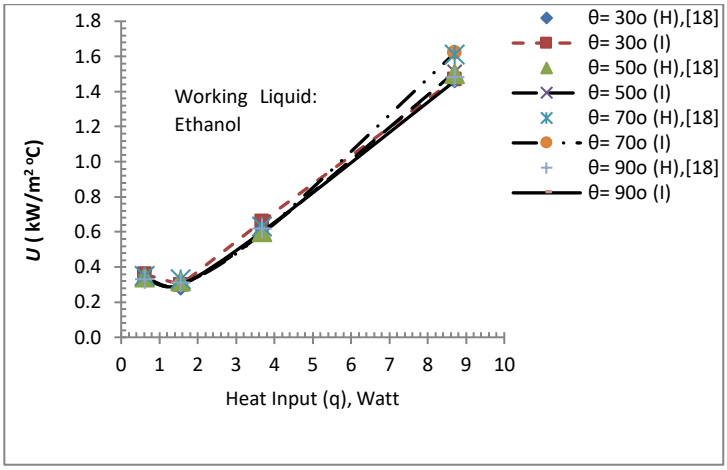

Figure 23 Validation experiment with the known results [18]

The variation of overall heat transfer coefficient, *U*, at different inclinations are shown in the following figures, Fig.3.10 (a-d). In the legendry of the plots, H represents Hossain et al [18] and I for Iqbal (author).

Uncertainty Analyses

A detailed analysis regarding the uncertainties within the equipment, measurements and results is carried out, which cumulatively is 8.90% with 95% confidence level, According to Kline and McClintock [19] the total uncertainty propagation for $r = f(v_{j=1\ldots n})$ is summarized in *eqn. 1* which is commonly used in calculating the related uncertainties in any experiment.

$$u(r) = \sqrt{\sum_{j=1}^{n}[\frac{\partial r}{\partial v_j}u(v_j)]^2} \ldots\ldots\ldots (1)$$

Here, *u* stands for the standard uncertainty, which is equivalent to the standard deviation, and v_j stands for the variables that contribute to the uncertainty in the result *r* that revolves around any data reduction equation. Thus finally, the relative uncertainties for *h* can be cumulatively expressed as in *eqn. 2*

$$\left(\frac{U_h}{h}\right)^2 = \left\{\left(\frac{U_{h_e}}{h_e}\right)^2 + \left(\frac{U_{h_a}}{h_a}\right)^2 + \left(\frac{U_{h_c}}{h_c}\right)^2\right\} \times 100\% \ldots\ldots\ldots (2)$$ or, it can be re-written for standard uncertainty in the form of *eqn. 1* as shown in *eqn. 3*.

$$u(h) = \left\{\sqrt{\sum_{j=e}^{c}\frac{\partial h}{\partial q_j}h(q_j) + \sum_{j=e}^{c}\frac{\partial h}{\partial T_j}h(T_j) + \sum_{j=e}^{c}\frac{\partial h}{\partial A_j}h(A_j)}\right\} \times 100\% \ldots\ldots\ldots (3)$$

where *j* = *e*, *a* and *c* which represents evaporator, adiabatic and condenser respectively.

Correlation

A dimensionless correlation has been developed which correlates all the data collected in this study. It is mentioned earlier and shown in the graphs that a few common relations are found between heat transfer coefficient and other operating parameters. These common relations may be shown mathematically as $h = f(\rho(p(q)))$

In a dimensionless relation, the above function can be rewritten along with the calculated constants as follows.

$$\frac{h}{h_{eff}} = 0.93\left(\frac{q"_{e,eff}}{q"_{e,s}}\right)^{0.731}\left(\frac{q"_{c,s}}{q"_{c,eff}}\right)^{0.014}\left(\frac{\Delta P}{\Delta P_{eff}}\right)^{0.863}\left(\frac{\rho_c}{\rho_e}\right)^{0.438}\left(\frac{d_T}{d_H}\right)^{1.000}\left(\left\{\frac{l}{l_{eff}}\right\}^{sin\theta cos\theta}\right)^{1.534}$$

Graphical representation of all the correlated data is shown in Figure 23, and 95% of them are found to be within ±15% range of the regression line.

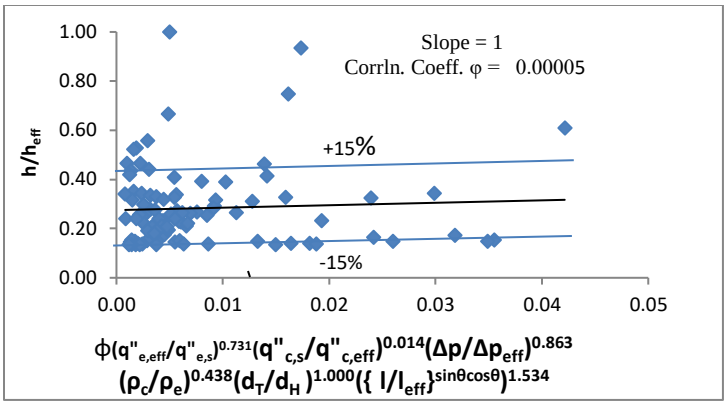

Figure 23. Graphical representation of the developed correlation of TMMHP

Conclusions

From the study, the following conclusions may be drawn:

(1) In SMMHP, the terminal temperature difference is very high comparing with that of in TMMHP. As a result, the *h* of the working fluid produced by the SMMHP is much smaller than that of TMMHP.

(2) Out of four working fluids, *methanol* has been found to be of the highest *h* because of its lowest boiling point that enables quick completion of thermodynamic cycle.

(3) Out of three orientations, TMMHP at 45_o produces the highest value of *h* for all four fluids; however, the sequence of *h* remains the same in all the orientations.

(4) It is proven that MHP made with the metals of variable thermal conductivity (i.e.TMMHP) of ascending order orientation, which initiates the super heater effect in the evaporator, indicates many folds better prospect of *h* value than that of made with constant conductivity (SMMHP).

(5) While an assumption of single phase flow in SMMHP works well at lower heat inputs, but at moderately high heat inputs it becomes a two-phase flow. However, the super heater effect at the evaporator in TMMHP eliminates that complexity of the two-phase and instantly turns into a single phase flow of vapor which was not possible in SMMHP [6, 7].

(6) In case of water, the upper trend of temperature at the condenser port is uniquely different from that of other liquids. Such a condition demands the coolant flow at lower than the ambient temperature or a coolant of higher C_p. Eventually, the slightly increased temperature of the vapor condensate speeds up the capillary action of the wick.

(7) Even though the values of *h* in TMMHP are many times higher than those of in SMMHP, the limitation of its value is obvious in both the heat pipes at a relatively higher heat input.

(8) The change of any specific physical property (i.e. density, specific gravity, viscosity) of a fluid singly cannot change the *h* of that fluid in an MHP, rather it is a compound value developed functionally from both of its physical properties and state variables.

Nomenclature

C_p, specific heat at constant pressure, $kJ/kg.^0C$

d_H, hydraulic diameter of the heat pipe, *(m)*

d_T, profile height of the heat pipe, *(m)*

h, heat transfer coefficient for terminal temperature difference of the fluid, $kW/m^{2.0}C$

h_{eff}, effective heat transfer coefficient for terminal average temperature difference of the fluid, $kW/m^{2.0}C$

l, length of the heat pipe, *m*

l_{eff}, effective length of the heat pipe, *m*

p, pressure of the fluid, *Pa* (N/m^2)

q, heat input, *Watt*

Δp, terminal pressure drop, *kPa*

Δp_{eff}, effective pressure drop at terminal average pressure, *kPa*

q'', heat flux, kW/m^2

$q''_{e,\,eff,}$ effective heat flux through the evaporator shell by conduction, kW/m^2

$q''_{e,\,s,}$ heat flux at the evaporator surface supplied by heater, kW/m^2

$q''_{c,\,s,}$ dissipated heat flux from the condenser surface by convection cooling, kW/m^2

$q''_{c,\,eff}$, effective heat flux dissipated through the condenser shell by conduction, kW/m^2

R_{eff}, effective thermal resistance, $^o C/Watt$

T_1-T_5, temperatures of the fluids in the micro heat pipe, ^0C

ρ, density of the fluid, kg/m^3

ρ_c, density of the fluid at the condenser, kg/m^3

ρ_e, density of the fluid at the evaporator, kg/m^3

φ, dimensionless correlation constant

θ, angle of inclination, degree (^{o})

Subscripts:

c,	condenser
e,	evaporator
eff,	effective
p,	constant pressure
s,	surface of the heat pipe
1-5,	positions of thermocouples

Conflict of Interest: The authors hereby confirm that no conflict of interests arises in conducting this research work.

References

[1] G. P. Peterson, "An Introduction to Heat Pipes-Modeling, testing and applications", John Wiley & Sons, Inc., 1994.

[2] G. M. Grover, T. P. Cotter and G. F. Erickson, "Structures of Very High Thermal Conductance", Journal of Applied Physics, 35(6): 1990-1991, 1964.

[3] P. D. Dunn and D. A. Reay, "Heat pipes", 3rd Edition, Publisher: Robert Maxwell, Chapter 1-5, 1982.

[4] T. N. Sreenivasa, S. N. Sridhara and G. Pundarika, "Working fluid inventory in miniature heat pipe", Proceedings of the International Conference on Mechanical Engineering (ICME'05), Dhaka, Bangladesh, 2005.

[5] M. A. R. Akhanda, S.L.Mahmood and Ashik Ahmed, "An experimental investigation of an air-cooled miniature heat pipe (MHP) using different working fluids at different fill ratios", Proceedings of the 3rd BSME-ASME International Conference on Thermal Engineering, Dhaka, Bangladesh, Paper No. BA 175, 2006.

[6] S. L. Mahmood, "Experimental Investigation on Micro Heat Pipes of Different Cross-sections having same Hydraulic Diameter", MS Thesis, Islamic University of Technology, OIC, Bangladesh, September 2007.

[7] A. S. Annamalai and V. Ramalingam, "Experimental investigation and computational fluid dynamics analysis of an air cooled condenser heat pipe", THERMAL SCIENCE, 15(3): 759-772, 2011.

[8] KMN S. Iqbal, "Thermal performances of two-metal (Cu-Ag) micro heat pipe (TMMHP)", Ph.D. Thesis, Islamic University of Technology, OIC, Bangladesh, November 2014.

[9] S. H. Moon**, "**Improving Thermal Performance of Miniature Heat Pipe for Notebook PC Cooling",pages:135-140, January 2002.

[10] B. R. Babin, G. P. Peterson, and D.Wu, "Steady-state Modeling and Testing of a Micro Heat Pipe," *J. Heat Transfer*, Vol. 112, 595-601,1990.

[11] S. W. Chi, "Heat Pipe Theory and Practice,"McGraw-Hill, NY, U.S.A., 1976.

[12] J. Longtin, B. F. Badran, and M. Gerner, "A One-dimensional Model of a Micro Heat Pipe during Steady-state Operation," J. Heat Transfer, Vol. 116, 709-715,1994.

[13] L. W. Swanson and G. P. Peterson, "The Interfacial Thermodynamics of the Capillary Structures in Micro Heat Pipes," J. Heat Transfer, Vol.17, pp. 195-201,1995.

[14] D. Wu and G. P., Peterson,"Investigation of the Transient Characteristics of a Micro Heat Pipe," J. Thermophysics, Vol. 5,129-134, 1991.

[15] M. Le Berre, G. Pandraud, P. Morfouli, and M. Lallemand," The performance of micro heat pipes measured by integrated sensors". Journal of Micromechanics and Microengineering, 16:1047–1050, 2006.

[16] Madhusree Kole and Dev, "Thermal performance of screen mesh wick heat pipes using water based copper nanofluids", Last visited on June 02, 2014.

[17] Yuan-Ching Chiang**,** Jen-Jie Chieh and Chia-Che Ho,**"**The magnetic-nanofluid heat pipe with superior thermal properties through magnetic enhancement", Last visited on June 02, 2014.

[18] Hossain, R.A., Chowdhuri, M.A.K, Feroz, C. M.,"Design, Fabrication and Experimental Study of Heat Transfer Characteristics of a Micro Heat Pipe",Jordan Journal of Mechanical and Industrial Engineering, Volume 4, Number 5, Pages 531- 542, 2010.

[19] Kline, S. J. and McClintock, F. A.,"Describing the uncertainties in single sample experiments". Mechanical Engineering, pages 3–8, 1953.

[20] L. Bai, J. Guo, G. Lin, J. He and D. Wen,"Steady-state modeling and analysis of a loop heat pipe under gravity-assisted operation", Applied Thermal Engineering, Volume 83, pp 88-97, 2015.

[21] Y. Li, J. He, H. He, Y. Yan, Z. Z, Bo, Li, "Investigation of ultra-thin flattened heat pipes with sintered wick structure", Applied Thermal Engineering, Volume 86, pp 106-118, 2015.
[22] S. Wu, T. Gu, D. Wang and Y. Chen, "Study of PTFE wick structure applied to loop heat pipe", Applied Thermal Engineering, Volume 81, April 2015, pp 51-57.
[23] KMN S. Iqbal and M. A. R. Akhanda, "Study of two-metal (Cu-Ag) micro heat pipe of convergent-divergent circular cross section using different working liquids of low boiling point", Global Journal of Researches in Engineering: J, General Engineering,Vol.15/1, 2015.
[24] KMN S. Iqbal and M. A. R. Akhanda, "Studly of two-metal (Cu-Ag) micro heat pipe of square cross section using differet liquids of low boiling point",Vol.2/3, pp 82-92.
[25] Yamamoto, K., Nakamizo, K., Kameoka, H. and Namba, K., 2002, "High Performance Micro Heat Pipe", Furukawa review No. 27, pp. 3-8.

Acknowledgement: The authors gratefully acknowledge the total financial along with other necessary supports in conducting this research provided by the Islamic University of Technology (IUT), OIC, Bangladesh.